Theor Chim Acta (1994) 88: 13–27

Theoretica Chimica Acta

The performance of energy extrapolation procedures in truncated averaged coupled-pair functionals*

Jörg Jenderek and Christel M. Marian
Institute of Physical and Theoretical Chemistry, Unversity of Bonn, Wegelerstraße 12, D-53115 Bonn, Germany

Received December 7, 1992/Accepted July 9, 1993

Summary. Energy extrapolation techniques in conjunction with individual configuration selection are applied to averaged coupled-pair functional expansions. In order to test the quality of this approach, benchmark calculations have been performed for N_2, the open and ring forms of O_3, and for the ground and several excited states of CuH and PdH. Reliable energy estimates are obtained for N_2 and the two transition metal hydrides and spectroscopic properties are in close agreement with the values for the non-truncated expansions. In the case of O_3 the perturbation corrections substantially underestimate the complete singles and doubles results. These deviations cancel to a large extent, however, in the calculated isomerization energy. The accuracy of the one-particle density matrix is examined by computing dipole moments for several electronic states of CuH and PdH. Deviations are significant in some cases. For the evaluation of properties the current approach requires modifications.

Key words: Averaged coupled-pair functionals – Energy extrapolation

1 Introduction

The averaged coupled-pair functional (ACPF) approach developed by Gdanitz and Ahlrichs [1] is a well-established method in quantum-chemical investigations aiming at spectroscopic accuracy. It combines the qualities of a multireference method with approximate size-extensivity. As already pointed out by Gdanitz and Ahlrichs [1], the ability to solve the ACPF equations is easily implemented into existing multireference single and double excitation configuration interaction (MRCI) codes. Following the ideas of Gershgorn and Shavitt [2] and of Buenker and Peyerimhoff [3, 4], we have applied configuration selection and energy extrapolation techniques within the ACPF approach. We have investigated whether it is possible to apply and join the advantages of both: to maintain the approximate size-extensivity of the ACPF and better agreement with full CI (FCI)

* Dedicated to Prof. W. Kutzelnigg on the occasion of his sixtieth birthday

as compared to MRCI approaches on the one hand, and to take advantage of the lower expense and higher flexibility of individually selected configuration expansions.

First test calculations were carried out for the ground state of N_2 in a double zeta plus polarization (DZP) atomic orbital (AO) basis for which FCI results are available [5]. We have studied the sensitivity of the extrapolated energies with respect to the number of secular equations on which the extrapolation procedure is based and have examined the accuracy of the energy extrapolation as a function of the configuration selection threshold. For comparison, these studies were performed both for ACPF and MRCI expansions.

A more realistic test case are transition metal compounds for which the ACPF method has been widely used. Size-extensivity is important not only for the computation of dissociation energies but also for excitation energies between states with differing *d* occupations. The charge distribution and consequently properties like the dipole moment are very sensitive to a balanced description of atomic channels and the ACPF method has been found to give the best results so far for dipole moments in transition metal compounds [6, 7]. For the transition metal hydrides CuH and PdH we have studied the performance of truncated ACPF expansions on spectroscopic properties derived from the (extrapolated) energies, e.g., bond distances, vibrational frequencies, excitation energies, etc., but also on the dipole moment which should give some clues concerning the convergence of the one-particle density matrix.

Our final test system is a typical example in which near-degeneracies play a major role, namely the isomerization energy for the open and cyclic forms of ozone.

2 Theory

For various electron correlation approaches the correlation energy can be obtained by minimizing the functional [8]:

$$\Delta E^c = \frac{\langle \Psi^0 + \Psi^c | \hat{H} - E^0 | \Psi^0 + \Psi^c \rangle}{\langle \Psi^0 | \Psi^0 \rangle + g \cdot \langle \Psi^c | \Psi^c \rangle} \stackrel{!}{=} \text{Minimum}, \tag{1}$$

which results in an eigenvalue matrix equation:

$$(\hat{H} - E^0)(\Psi^0 + \Psi^c) = \Delta E^c \hat{G}(\Psi^0 + \Psi^c), \tag{2}$$

$$\text{with} \quad \hat{G} = |\Psi^0\rangle\langle\Psi^0| + g|\Psi^c\rangle\langle\Psi^c|$$

$|\Psi^c\rangle$ denotes the correlation function orthogonal to the reference wavefunction $|\Psi^0\rangle$. E^0 designates the reference energy $\langle\Psi^0|H|\Psi^0\rangle$. The factor g is equal to 1 for the MR-SDCI functional. In the original work of Gdanitz and Ahlrichs [1] different g values were used for different parts of the correlation function: $g = 1$ was chosen for valence space configurations, i.e., those in which no external orbital is occupied, and for the others a factor of $2/N$ was proposed where N is the number of correlated electrons. Following the choice of g in the implementation of the ACPF procedure within the MOLECULE-SWEDEN program package [9] by Blomberg, a factor of $2/N$ was employed for all parts of the correlation function. An estimate for the ACPF energy may be obtained by performing MRCI

calculations and adding the Pople correction [10] (sometimes also called ACPF correction):

$$A\cdot(1-g)\cdot(1-C_0^2)\Delta E_{\mathrm{MRCI}} \quad \text{with} \quad A=1/(C_0^2+g(1-C_0^2)) \tag{3}$$

to the variationally determined energy.

The one-particle density matrix for the evaluation of properties is built according to the prescription [8] that the trace of the product of the density matrix and the one-particle integrals should equal the one-electron energy. In the present notation γ_{ACPF} is given by

$$\gamma_{\mathrm{ACPF}}=1/C_0^2(1-A)(\Psi^0)+A\gamma(\Psi^0+\Psi^c). \tag{4}$$

According to second-order Epstein–Nesbet perturbation theory [11, 12] the correlation energy contribution of a configuration state function (CSF) $|\Psi_j\rangle$ to the reference wavefunction $|\Psi^0\rangle$ can be estimated as

$$|\Delta\varepsilon_j^c|=\frac{|\langle\Psi^0|\hat{H}|\Psi_j\rangle|^2}{E^0-\langle\Psi_j|\hat{H}|\Psi_j\rangle} \tag{5}$$

The energy lowering $|\Delta\varepsilon_j^c|$ has been proposed to serve as a selection criterion [2]: all single and double excitations with an energy contribution $|\Delta\varepsilon_j^c|$ exceeding a prechosen threshold T are included in the secular equation to be solved variationally (Eq. (2)). The influence of all other CSFs on the energy is taken into account by a correction term:

$$\Delta\mathscr{E}(T)=\sum_{\{j:\,|\Delta\varepsilon_j^c|\le T\}}\Delta\varepsilon_j^c. \tag{6}$$

If second-order Epstein–Nesbet perturbation theory were a good approximation to the unselected problem the sum of the eigenvalues and the correction term should nearly equal the unselected energy independent of the selection thresholds.

$$E(T)+1\cdot\Delta\mathscr{E}(T)\approx E(T=0) \quad \text{for all } T. \tag{7}$$

This is often not the case and Buenker and Peyerimhoff [4] proposed to employ a two-point linear extrapolation of this sum as an estimate of the zero-threshold energy, instead.

$$E(T\to 0)=E(T_1)+\lambda_{\mathrm{opt.}_2}\Delta\mathscr{E}(T_1) \quad \text{with} \quad \lambda_{\mathrm{opt.}_2}=-\frac{E(T_1)-E(T_2)}{\Delta\mathscr{E}(T_1)-\Delta\mathscr{E}(T_2)}. \tag{8}$$

In addition to this zero-threshold estimate, we use an n-point weighted linear regression:

$$E(T\to 0)=\left(n\sum_{k=1}^{n}\frac{E(T_k)}{\Delta\mathscr{E}(T_k)^2}-\sum_{k=1}^{n}\frac{1}{\Delta\mathscr{E}(T_k)}\sum_{k'=1}^{n}\frac{E(T_{k'})}{\Delta\mathscr{E}(T_{k'})}\right)\Big/\mathrm{DET} \tag{9}$$

with

$$\mathrm{DET}=n\sum_{k=1}^{n}\left(\frac{1}{\Delta\mathscr{E}(T_k)}\right)^2-\left(\sum_{k=1}^{n}\frac{1}{\Delta\mathscr{E}(T_k)}\right)^2 \tag{10}$$

which is equal to Eq. (8) for $n=2$.

The truncated ACPF procedure was implemented [13] into the MRD-CI program package [14]. Molecular orbitals (MOs) were calculated employing the MOLECULE-SWEDEN programs [9] which were interfaced [15] to both the

Table 1. Energy differences ΔE with respect to FCI energies[a] for the $^1\Sigma^+$ ground state of N_2 employing CASSCF MOs

Internuclear separation		2.1	3.0	4.0	50.0
Method	T^{bc}	$\Delta E_{T\to 0}^{n=2} = E_{FCI} - E_{T\to 0}^{n=2}$ [d]			
CASSCF		+ 0.055898	+ 0.057118	+ 0.048096	+ 0.040735
MRCI	10	+ 0.002001	+ 0.001952	+ 0.000699	+ 0.000564
MRCI	1	+ 0.000920	+ 0.001082	+ 0.000684	+ 0.000564
MRCI	0	+ 0.000761	+ 0.000869	+ 0.000664	+ 0.000487
ACPF	10	+ 0.001430	+ 0.001146	+ 0.000073	+ 0.000156
ACPF	1	+ 0.000317	+ 0.000223	+ 0.000040	+ 0.000156
ACPF	0	+ 0.000150	− 0.000013	+ 0.000017	+ 0.000073

[a] FCI energies according to Bauschlicher et al. [5]
[b] T is the CSF selection threshold value in units of 10^{-6} E_H (microhartree)
[c] $\Delta T = T$ is the threshold increment
[d] In units of E_H (extrapolated out of 2 data points according to Eq. (8))

MRD-CI and the COLUMBUS program systems [16]. Direct CI/ACPF calculations were carried out using either the COLUMBUS or the MOLECULE-SWEDEN suite of programs. All calculations were performed on the Convex 220 of the "Sonderforschungsbereich 334" at the University of Bonn.

3 Applications

3.1 The nitrogen molecule

N_2 is a typical test molecule for correlation methods. Because of its triple bond a proper description of the dissociation process must take care of correlation effects. FCI benchmarks [5, 17] make it possible to compare and judge the different methods.

Following the lines of Bauschlicher et al. [5] we calculated complete active space self-consistent field (CASSCF) [18] energies at various atomic distances. The AO basis (DZP) is the same as applied by these authors. 14 configurations (20 CSFs) is the minimal set which allows a qualitatively correct description of the bond breaking. With these references MRCI and ACPF wavefunctions for various selection thresholds T have been computed. In Table 1 the differences of the extrapolated energies with respect to the FCI energies are shown.

The ACPF energies are in good accord with the FCI energies. An improvement with respect to MRCI values is observed for all distances and selection thresholds. In order to visualize the influence of the configuration selection and extrapolation procedures on the accuracy of the resulting energies, eigenvalues and energies including various perturbational estimates are shown in Figs. 1 and 2 as a function of the selection threshold. We have plotted the data for a bond distance of 2.1 a_0 since the perturbational corrections are largest at small internuclear separations. The curves at longer bond distances are similar but have smaller gradients and the variations of the extrapolated values are more damped.

As one can see from Figs. 1 and 2 the configuration selection and energy extrapolation has nearly the same effect on both ACPF and MRCI methods, the ACPF curves being shifted toward lower energies. For the wavefunctions

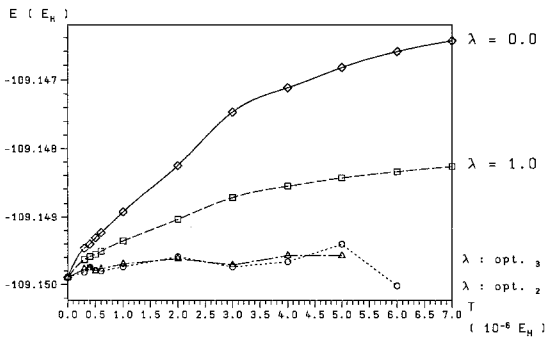

Fig. 1. MRCI energies of N_2 at $R = 2.1\ a_0$ using CASSCF MOs. The topmost curve (*diamond markers, solid line*), labeled $\lambda = 0.0$, displays the eigenvalues of the secular equations. The graph (*square markers, dashed line*) designated $\lambda = 1.0$ is obtained by adding the unmodified perturbation sum (Eq. (6)) to the corresponding eigenvalue. Employing a linear extrapolation based on the energies at 2 neighboring threshold values (Eq. (8)) results in a curve (*circled markers, short dashed line*) named λ: opt.$_2$. Linear regression using 3 data points (*triangular markers, dotted dashed line*) is marked with λ: opt.$_3$

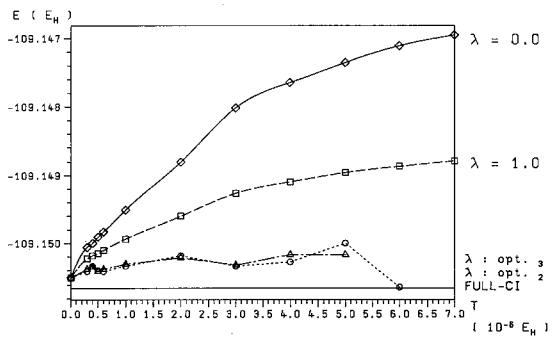

Fig. 2. ACPF energies of N_2 at $R = 2.1\ a_0$ using CASSCF MOs. Explanation of symbols see Fig. 1. In addition the FCI energy is displayed (*no markers, solid line*), which amounts to $-109.150642\ E_H$ [5]

optimized in a basis of CASSCF orbitals (Figs. 1 and 2) and selection thresholds below $5 \times 10^{-6}\ E_H$ the extrapolation error is less than $2 \times 10^{-4}\ E_H$, one order of magnitude smaller than the perturbational correction of the eigenvalue. Using a 3-point weighted linear regression (Eq. (9)), makes the final energies even less sensitive. They are nearly independent of the number of data points which have been used for the extrapolation in these cases. It should be noted that on an absolute scale the energy differences of the extrapolated ACPF energies to the FCI energies are comparatively small. The size of the deviations obtained in the present work is in the same ballpark as those of the FCI estimates by Cave et al. [19]. On the other hand, the results of recent applications of generalized Møller–Plesset and of Epstein–Nesbet perturbation theories on N_2 [20], employing the same basis set parameters as in the present study, show considerably larger errors.

3.2 Copper hydride

The computation of the correlation energy is very demanding for compounds of the late transition metals. Because of the higher electron correlation in the compact 3*d* shell as compared to 4*s*, *d*-electron-rich states are expected to be preferentially

Table 2. Total energies E [E_H] (offset -1653), excitation energies ΔE [eV], and dipole moments μ [ea_0] for various electronic states of CuH at $R_{CuH} = 2.9\ a_0$

Method	Property	$1\,^1\Sigma^+$	$1\,^3\Pi$	$1\,^3\Pi$	$1\,^3\Delta$	$1\,^1\Delta$
$MRCI_s$[a]	E	−0.941024	−0.849364	−0.839767	−0.846033	−0.840984
MRCI	E	−0.942886	−0.850591	−0.840566	−0.847464	−0.841945
$MRCI_s^{+Q}$[a,b]	E	−0.965145	−0.865934	−0.857298	−0.862773	−0.858495
$MRCI^{+Q}$[a]	E	−0.968216	−0.869440	−0.859793	−0.866581	−0.861225
$ACPF_s$[a]	E	−0.970062	−0.871324	−0.861974	−0.867996	−0.863116
ACPF	E	−0.973246	−0.873479	−0.863799	−0.871005	−0.865286
$MRCI_s$[a]	ΔE	0.00	2.50	2.77	2.59	2.72
MRCI	ΔE	0.00	2.51	2.78	2.60	2.75
$MRCI_s^{+Q}$[a,b]	ΔE	0.00	2.70	2.93	2.78	2.90
$MRCI^{+Q}$[a]	ΔE	0.00	2.69	2.95	2.77	2.91
$ACPF_s$[a]	ΔE	0.00	2.69	2.94	2.78	2.91
ACPF	ΔE	0.00	2.71	2.98	2.78	2.94
$MRCI_s$[a]	μ	1.2715	0.1822	0.1111	0.2045	0.0536
MRCI	μ	1.2368	0.1586	0.0906	0.1808	0.0333
$ACPF_s$[a]	μ	1.1668	0.1911	0.1375	0.2189	0.0659
ACPF	μ	1.0461	0.1442	0.1017	0.1586	0.0265

[a] Calculations with configuration selection and energy extrapolation
[b] Including unlinked cluster correction according to Pople [10]

stabilized when a higher percentage of the correlation energy is recovered in the calculations. The $X\,^1\Sigma^+$ state of CuH originates from the ground state dissociation products $Cu(^2S_g) + H(^2S_g)$ and has a d occupation of almost 10 electrons. The excited $^3\Pi$, $^1\Pi$, $^3\Delta$, and $^1\Delta$ states have predominately d^9 character and emerge from copper in its $d^9s^2(^2D_g)$ state. For further details the reader is referred to Ref. [21].

The AO basis set is the [9*s*7*p*4*d*3*f*/4*s*3*p*] GTO basis used in recent work [21]. All calculations are performed at an internuclear separation of 2.9 a_0. Relativistic (one-component) CASSCF orbitals are chosen as one-particle basis sets, where for the upper states six active electrons are distributed among three active σ orbitals and the π_x and π_y orbitals ($^1\Pi$, $^3\Pi$) or $\delta_{x^2-y^2}$ and δ_{xy}($^1\Delta$, $^3\Delta$) orbitals, respectively. In the ground state the active space comprises four σ orbitals in which four active electrons are distributed. In the ACPF step 12 electrons are correlated with three and four configurations spanning the reference space for the ground and excited states, respectively. The CSF selection threshold amounts to 5×10^{-6} E_H in the truncated ACPF calculations while single excitations to the leading reference configuration are retained irrespective of their energy contributions. The non-truncated MRCI and ACPF results were obtained using the MOLECULE-SWEDEN programs.

In Table 2 the results of our calculations on various electronic states of CuH is presented. The MRCI values and the results of the complete singles and doubles ACPF are taken from Ref. [21].

Let us focus on energies first. Extrapolated energies are found to be close to the zero-threshold values. Absolute energies differ by 1 to 3 mh (millihartrees), with the

deviation being slightly larger for ACPF than for MRCI. Excitation energies agree even better with the results for the corresponding complete singles and doubles treatment since the perturbation theory estimate is consistently above the true values. As expected, the methods including unlinked cluster corrections lower preferentially the ground state so that the relative energies for the family of d^9 states is shifted uniformly to higher values. Comparing ACPF energies and MRCI energies with the Pople correction (Eq. (3)) added it is observed that absolute ACPF energies are 4 to 5 mh lower while relative energies are nearly equal.

The agreement of the dipole moments obtained from truncated and nontruncated MRCI wavefunctions is quite satisfactory in the case of copper hydride. The largest deviation is found for the ground state where the difference is in the order of $0.04\ ea_0$. The convergence of the one-particle density matrix for the truncated ACPF expansion is less convincing, as reflected in the dipole moments. This is particularly apparent for the ground state of CuH. While the dipole moment for the non-truncated ACPF is essentially reduced by $\approx 0.2\ ea_0$ or ≈ 0.5 D with respect to the MRCI value, the values are much closer for the truncated expansions. The effect of the unlinked cluster corrections on the dipole moments are considerably underestimated in the latter case.

3.3 Palladium hydride

Palladium hydride is the next heavier homolog of nickel hydride. Both compounds have a low-lying $^2\Delta$, $^2\Pi$ and $^2\Sigma^+$ state. While the ordering of states is $^2\Delta < ^2\Sigma^+ < ^2\Pi$ in NiH [22], PdH has a $^2\Sigma^+$ ground state [23]. The locations of $^2\Delta$ and $^2\Pi$ are not yet known experimentally. Previous theoretical studies [24–26] find excitation energies (not including spin–orbit coupling) of about 4500–6800 cm^{-1} for the $^2\Delta$ state and approximately 7900–8700 cm^{-1} for $^2\Pi$. Employing a one-component relativistic (no-pair) Hamiltonian [27] we have investigated the three low-lying states of palladium hydride. Special attention has been payed to the effect on spectroscopic properties brought about by truncating the ACPF expansions.

The AO basis set on Pd comprises $(17s13p9d4f)$ primitive Gaussian functions [28] which were contracted in relativistic atomic calculations on the $d^9s^1(^3D_g)$ state to $[12s9p6d3f]$. The $[4s3p1d]$ hydrogen basis is the same as in a recent study on NiH [6]. The CASSCF active space includes four σ orbitals for $^2\Sigma^+$ and the d_π or d_δ orbitals for $^2\Pi$ and $^2\Delta$, respectively. The number of active electrons is $3(^2\Sigma^+)$ or $5(^2\Pi$ and $^2\Delta)$. 10 reference configurations were found to be important for the $^2\Sigma^+$ ground state, while the reference set of the excited states comprised 8 configurations. The selection threshold for truncating the ACPF expansions was set to $10^{-6}\ E_H$ with a threshold increment of $5 \times 10^{-7}\ E_H$ and three secular equations used for the energy extrapolations. Single excitations to the leading reference configuration were retained throughout. The non-truncated ACPF calculations were performed with the MOLECULE-SWEDEN programs. Our results for the equilibrium bond distances, vibrational frequencies and excitation energies for the $^2\Sigma^+$, $^2\Delta$ and $^2\Pi$ states of palladium hydride are given in Table 3. These properties were determined from 5th degree polynomial fits (the lowest exponent being -1) to the calculated data points. Dissociation energies are computed with respect to the atomic $d^{10}(^1S_g)(^2\Sigma^+)$ and $d^9s^1(^3D_g)$ states ($^2\Delta$ and $^2\Pi$). The energies of the atomic states are obtained from single-reference calculations employing SCF orbitals.

Table 3. Spectroscopic properties of low-lying electronic states of PdH

State	Method	R_e [Å]	ω_e [cm^{-1}]	T_e [cm^{-1}]	D_e [eV]
$^2\Sigma^+$	$ACPF_s$[a]	1.533	2027	0[b]	2.25
$^2\Sigma^+$	ACPF	1.534	1997	0	2.38
$^2\Delta$	$ACPF_s$[a]	1.627	1745	7031	2.22
$^2\Delta$	ACPF	1.619	1803	7308	2.34
$^2\Pi$	$ACPF_s$[a]	1.696	1606	8971	1.98
$^2\Pi$	ACPF	1.685	1654	9250	2.09

[a] Calculations with configuration selection and energy extrapolation
[b] The difference of energy to the non-truncated calculation is 1240 cm^{-1}

The extrapolation procedure is found to give equilibrium bond distances and adiabatic excitation energies in very good agreement with the zero-threshold values. Potential curves for extrapolation estimates and non-truncated expansions run essentially parallel. This may be seen from Fig. 3 where potential curves are displayed for the $X^2\Sigma^+$ ground state or even more clearly from Fig. 4 where the energy differences with respect to the unselected ACPF calculations for all three states have been plotted. These energy difference plots are more or less straight lines, the upper ones corresponding to the eigenvalues of the truncated expansions, the lower ones belonging to the extrapolated ACPF energies.

Two irregularities among the $X^2\Sigma^+$ extrapolated energies are observed at internuclear separations around 3.0 and 3.3 a_0. No such data scatter is found for the $^2\Delta$ and $^2\Pi$ states. The irregularities occur both for the extrapolated MRCI and ACPF energies whereby the deviations are more marked in the ACPF case. We have traced down the origin of this behavior to the sensitivity of the extrapolation procedure to potential energy curve crossings. As apparent from Fig. 3 the corresponding energy expectation values of the truncated expansions fit smoothly to the potential curves. At a bond distance around 3.0 a_0 the second and third $^2\Sigma^+$ states undergo an avoided crossing. These states are located vertically about 3 eV above the ground state and are derived from Pd $d^9s^1(^1D_g)$ and d^9 configurations containing a strongly occupied $5p_\sigma$ orbital. At 3.3 a_0 a second avoided crossing occurs, this time with the d^{10} state which eventually becomes the ground state. Similar problems were encountered earlier for the ground and first excited $^1\Sigma^+$ states of CuH and could be remedied by merging the selected configuration spaces for various bond distances and keeping this merged configuration space fixed in the subsequent CI calculations [21].

Our ACPF excitation energies for the $^2\Delta$ and $^2\Pi$ are somewhat larger than those of earlier theoretical investigations [24–26] which is due to the improved correlation treatment of the ground state in the present work. The energy extrapolation underestimates the excitation energies only slightly ($\approx$300 cm^{-1}) which is consistent with the fact that the ground state exhibits a d population of approximately 9.2 electrons and requires higher computational effort than the $^2\Delta$ and $^2\Pi$ states with d populations of only 8.7 electrons. Harmonic vibrational frequencies evaluated from the extrapolated and zero-threshold energies are found to be in reasonable agreement.

In Fig. 5 the dipole moment functions of the PdH ground state are displayed for various methods. As also found for copper hydride (see above) and nickel hydride [6, 7] the ACPF approach yields a considerably smaller dipole moment value than

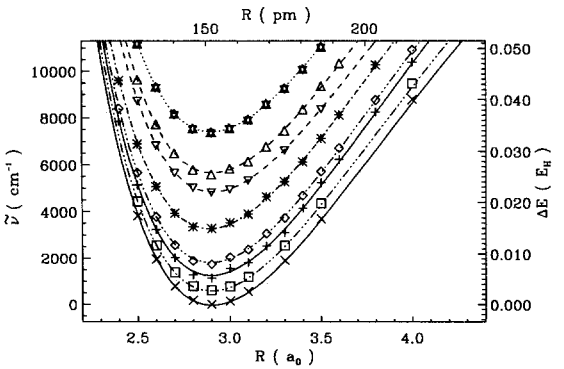

Fig. 3. Energies for the $X\,^2\Sigma^+$ ground state of PdH employing (un)-selected MRCI-calculations and (un)-selected ACPF-calculations; ⋆ $MRCI_s$ without extrapolation (*star, dotted line*); △ $MRCI_s$ (*triangle, dashed line*); ▽ MRCI (*inverse triangle, dashed line*); ∗ $ACPF_s$ without extrapolation (*asterisks, shortdashed-dashed line*); ◇ $MRCI_s^{+Q}$ (*diamonds, dashed-dotted line*); + $ACPF_s$ (*cross, solid line*); □ $MRCI^{+Q}$ (*squares, dashed-dotted line*); × ACPF (×, *solid line*)

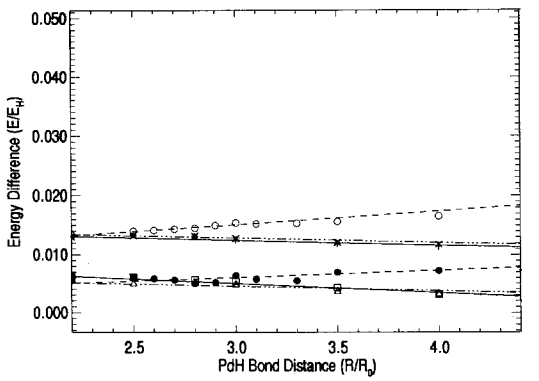

Fig. 4. Energy differences with respect to unselected ACPF calculations.
○ $^2\Sigma^+$ truncated, no extrapolation;
× $^2\Delta$ truncated, no extrapolation;
+ $^2\Pi$ truncated, no extrapolation;
● $^2\Sigma^+$ extrapolated ACPF energies;
△ $^2\Delta$ extrapolated ACPF energies;
□ $^2\Pi$ extrapolated ACPF energies

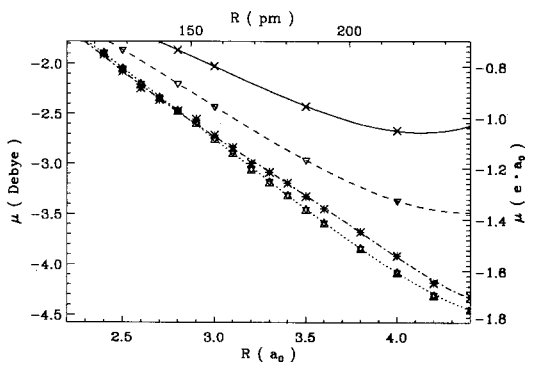

Fig. 5. Dipole moments for the $X\,^2\Sigma^+$ ground state of PdH employing (un)-selected MRCI-calculations and (un)-selected ACPF-calculations. Explanation of symbols see Fig. 3

the MRCI treatment. This is not the case for the truncated MRCI and ACPF expansions for which essentially equal values are obtained, almost 50% larger than the dipole moment for the non-truncated ACPF. It should be mentioned that the errors are smaller in the case of the excited states. It is conceivable that a B_k-type perturbation correction [2] which was found to work satisfactorily for hyperfine-coupling constants obtained from truncated MRCI expansions [29]

could remedy these shortcomings. Work to implement B_k-type corrections in the ACPF program is in progress.

3.4 Ozone

Ozone constitutes a somewhat more subtle test system. Its quantum-chemical treatment is complicated by the presence of various near-degenerate valence orbitals. Ozone has a $^1A_1$ electronic ground state with the energetically most favorable structure being an isosceles triangle with a bond angle of roughly 120 degrees. Due to a conical intersection with the second $^1A_1$ state [30] the ground state potential surface exhibits a second minimum at smaller bond angles. In terms of MO theory the existence of a $X\,^1A_1$ double well potential is easily rationalized. Among the MOs primarily composed of oxygen $2p$ orbitals, two in-plane orbitals ($3a_1', 3e'$) and two π-type out-of-plane orbitals ($1a_2'', 1e''$) are strongly occupied in the equilateral configuration. With increasing bond angle, the b_1 component of the doubly degenerate π-type HOMO $1e''$ is destabilized to become eventually the $2\pi_u$ antibonding orbital (together with $6a_1$) in the linear arrangement of the nuclei. The opposite behavior is observed for the b_2 component of the LUMO $4e'$. This in-plane orbital is stabilized upon ring opening and becomes the HOMO at the global minimum of the $X\,^1A_1$ hypersurface. In the linear conformation this $4b_2$ and the $1a_2$ orbital form a degenerate pair, the $1\pi_g$ non-bonding orbital.

An experimental value for the energy difference between the two minima is not available. At the single determinant level, it is computed to be only 0.4 eV (see below). It appears, however, that for the accurate determination of the relative energetic location of the two potential wells a proper description of static and dynamic electron correlation is crucial [31, 32].

The actual calculations were performed using the C_{2v} molecular point group symmetry. Experiments find a bond angle of 116.8 degrees and an interatomic distance of 1.271 Å between the central and the terminal oxygens [33] for the global minimum of the $X\,^1A_1$ hypersurface. The exact geometrical structure of the second minimum is still controversial [30]. We employ the structural data optimized by Lee [32] in CCSD(T) calculations using a [$5s4p3d2f$] ANO basis, i.e., an equilateral triangle with an O–O bond distance of 1.444 Å. The atomic orbital basis used in this work consists of a $(14s9p6d4f)/[(4+1)s(3+1)p2d1f]$ ANO-basis [34] on each of the oxygens, where $(4+1)s$ and $(3+1)p$ means that we have decontracted the most diffuse s and p primitives, respectively. Molecular orbitals were optimized at the CASSCF level. For the open form of ozone the CASSCF active space contains all valence orbitals composed of the oxygen $2p$ orbitals, i.e., three orbitals of a_1 symmetry, two b_1 orbitals, three b_2 orbitals, and one orbital of a_2 symmetry. The six lowest-lying MOs ($1a_1, 1b_2, 2a_1, 3a_1, 2b_2, 4a_1$) are kept doubly occupied under orbital optimization (inactive). In the ring form of ozone convergence problems were encountered with this choice of the active space. The $2b_2$ MO was found to contain – besides an antibonding linear combination of $2s$ orbitals – also significant $2p$ contributions and was added to the active space together with its degenerate $4a_1$ counterpart.

In the subsequent CI and ACPF calculations all configurations with the weight $|c|$ of a corresponding CSF in the CASSCF expansion exceeding 0.05 were included in the reference. The reference space contains 14 configurations for the cyclic form and 11 for the open structure. Apart from the six $1s$ electrons, all electrons are correlated. Energy selection thresholds for truncating the CI/ACPF expansion

vary in the range between 2×10^{-5} and 2.6×10^{-6} E_H, the latter giving rise to secular equations in the order of 32,000 which is the present limit in our CI/ACPF program for the number of CSFs to be treated variationally. The complete singles and doubles CI and ACPF expansions comprise 2 835 914 CSFs for the open and 3 022 193 CSFs for the cyclic isomer of ozone. These calculations are performed using the direct CI/ACPF codes in the COLUMBUS program package.

Results of our calculations on the open form of ozone are presented in Table 4. Table 5 gives the corresponding quantity for the equilateral triangle. In Table 6 the isomerization energies for the two structures are displayed for various selection thresholds. The energies extrapolated from two or three secular equations, respectively, differ only slightly (a few tenths of a millihartree) and only the latter are compiled in the Tables. The use of even more data points in the extrapolation procedure does not lead to a further improvement since the perturbational estimates of additional points at bigger thresholds are less reliable and tend to spoil the accuracy.

All methods agree in finding that the open form of ozone is much more stabilized by inclusion of electron correlation than cyclic ozone. This is in accord with other theoretical work [30–32, 35–41]. The literature data on the isomerization energy scatter considerably, however, the values ranging from roughly 0.7 eV to about 1.5 eV. The ground state dissociation limit lies 26.1 kcal/mol $\approx$ 1.13 eV [42] above the zero vibrational level. It is thus not clear whether the ring form is only metastable with respect to dissociation into $O_2 + O$. The complete singles and doubles MRCI and ACPF treatments (no selection) in this work place the ring

Table 4. Results for the open form of ozone

Method	$T^a/\Delta T^b$	E^c	$\sum_j^{disc.} \Delta\varepsilon_j{}^d$	ΔE^e	C_0^2	CSFs[f]
SCF		− 4.357 330				1
CASSCF		− 4.587 792				666
MRCI	20.0/20.0	− 5.085 402	0.270 631	0.50	0.9252	5 659
MRCI	3.0/ 1.0	− 5.086 518	0.095 059	0.46	0.9106	29 007
MRCI	2.6/ 1.0	− 5.086 610	0.087 034	0.46	0.9099	31 879
MRCI	0.0/ 0.0	− 5.103 689		0.00	0.8943	2 835 914
MRCI+Q[g]	20.0/20.0	− 5.124 256	0.270 631	0.94	0.9252	5 659
MRCI+Q[g]	3.0/ 1.0	− 5.133 735	0.095 059	0.69	0.9106	29 007
MRCI+Q[g]	2.6/ 1.0	− 5.134 204	0.087 034	0.67	0.9099	31 879
MRCI+Q[g]	0.0/ 0.0	− 5.158 910		0.00	0.8943	2 835 914
ACPF	20.0/20.0	− 5.136 005	0.270 631	1.03	0.9106	5 659
ACPF	3.0/ 1.0	− 5.144 523	0.095 059	0.80	0.8867	29 007
ACPF	2.6/ 1.0	− 5.144 890	0.087 034	0.79	0.8855	31 879
ACPF	0.0/ 0.0	− 5.173 877		0.00	0.8464	2 835 914

[a] T is the CSF selection threshold value in units of 10^{-6} E_H

[b] ΔT is the threshold increment in units of 10^{-6} E_H

[c] Extrapolated energies; using $n = 3$ datapoints (Eq. (9)); energy offset is -220 E_H

[d] Sum over perturbation contributions of discarded CSFs in units of E_H

[e] Energy difference [eV] with respect to corresponding unselected calculation

[f] Number of configuration state functions treated variationally

[g] Including unlinked cluster correction according to Pople [10]

Table 5. Results for the cyclic form of ozone

Method	$T^a/\Delta T^b$	E^c	$\sum_j^{disc.} \Delta\varepsilon_j{}^d$	ΔE^e	C_0^2	CSFs[f]
SCF		− 4.342 718				1
CASSCF		− 4.543 262				2351
MRCI	20.0/20.0	− 5.047 660	0.237 820	0.28	0.9221	5364
MRCI	3.0/ 1.0	− 5.046 712	0.087 177	0.30	0.9105	25 291
MRCI	2.6/ 1.0	− 5.047 158	0.080 682	0.29	0.9100	27 619
MRCI	0.0/ 0.0	− 5.057 853		0.00	0.8968	3 022 193
MRCI$^{+Q,g}$	20.0/20.0	− 5.087 817	0.237 820	0.70	0.9221	5365
MRCI$^{+Q,g}$	3.0/ 1.0	− 5.093 260	0.087 177	0.55	0.9105	25 291
MRCI$^{+Q,g}$	2.6/ 1.0	− 5.094 033	0.080 682	0.53	0.9100	27 619
MRCI$^{+Q,g}$	0.0/ 0.0	− 5.113 426		0.00	0.8968	3 022 193
ACPF	20.0/20.0	− 5.099 376	0.237 820	0.66	0.9061	5364
ACPF	3.0/ 1.0	− 5.103 497	0.087 177	0.55	0.8872	25 291
ACPF	2.6/ 1.0	− 5.104 239	0.080 682	0.52	0.8862	27 619
ACPF	0.0/ 0.0	− 5.123 532		0.00	0.8580	3 022 193

Footnotes see Table 4

Table 6. Energy differences between the cyclic and open structure of ozone

Method	T^a	Isomerisation energy[b]	
	$[10^{-6}\ E_H]$	$[E_H]$	[eV]
SCF		0.014 612	0.40
CASSCF		0.044 530	1.21
MRCI	20.0	0.037 742	1.03
MRCI	3.0	0.039 806	1.08
MRCI	2.6	0.039 452	1.07
MRCI	0.0	0.045 836	1.25
MRCI$^{+Q,c}$	20.0	0.036 439	0.99
MRCI$^{+Q,c}$	3.0	0.040 475	1.10
MRCI$^{+Q,c}$	2.6	0.040 171	1.09
MRCI$^{+Q,c}$	0.0	0.045 484	1.24
ACPF	20.0	0.036 629	1.00
ACPF	3.0	0.041 026	1.12
ACPF	2.6	0.040 651	1.11
ACPF	0.0	0.050 345	1.37

[a] T is the CSF selection threshold value
[b] Energy differences between the cyclic and the open form of ozone
[c] Including unlinked cluster correction according to Pople [10]

form of ozone above the ground state dissociation products (Table 6). Since we have not performed a geometry optimization of the cyclic structure this finding is not conclusive, however. On the other hand, it is expected that an improved correlation treatment, especially the inclusion of higher excitations, preferentially stabilizes the obtuse angular isomer.

Before proceeding to the discussion of the performance of energy extrapolation we would like to comment on the complete singles and doubles treatments. The comparably low weights of the reference function in the MRCI and ACPF expansions indicate that the reference set is not converged. In the MRCI expansions no further outstanding coefficients could be detected, however. Similar problems were reported recently by Borowski et al. [43] in CASSCF/MRCI calculations on the open form of ozone. The analysis of the ACPF wavefunction indicates that excitations into the $7a_1$ and $5b_2$ valence orbitals, but also semi-external excitations into *d* orbitals are of importance. An increased number of reference configurations of valence-type could easily be handled by direct internally contracted CI [44] or ACPF approaches [45, 46]; the number of active orbitals that emerge from adding the most significant semi-externals to the reference set would probably go beyond the scope of present GUGA based programs, however. The fact that the ACPF energies are significantly lower than the MRCI energies including unlinked cluster corrections according to Pople (see Tables 4 and 5) might be an artefact of the small $|\Psi_0|$.

From Tables 4 and 5 it is apparent that the current extrapolation of the truncated MRCI and ACPF energies considerably underestimates the zero threshold values of ozone, whereby the deviations are much bigger than the differences between the energies obtained from the extrapolation procedures based on the solution of two or three secular equations, respectively. An indicator for a substantial uncertainty in the extrapolation is already the size of the perturbation sums, which are forbiddingly large at a selection threshold of 20×10^{-6} E_H and are still sizable for the smaller threshold values. The energy remainders with respect to the unselected calculations are especially noteworthy for the open form, i.e., they are in the order of 20 mh for MRCI and about 30 mh for the ACPF energies. The corresponding errors in the ring form amount to approximately 10 and 20 mh, respectively. Due to its inherent multi-configurational character, ozone apparently belongs to those cases – investigated earlier by Jackels and Shavitt [47] and more recently by Cave et al. [19] – for which Epstein–Nesbet-type perturbation theory significantly underestimates the correlation contribution of configurations which do not have a considerable direct interaction with the reference wavefunction. One possible solution to the problem would be to enlarge considerably the number of orbitals optimized in the MCSCF, e.g., to allow excitations into the correlation *d* orbitals, and consequently to increase the number of reference configurations.

Regarding the relative energy separation between the two forms shown in Table 6 we find that the extrapolation errors partly compensate. The isomerization energies are off by 6×10^{-3} $E_H \approx 0.18$ eV (MRCI) and 10×10^{-3} $E_H \approx 0.28$ eV (ACPF). Although these deviations appear to be modest, they are substantial when it comes to decide whether the ring form of ozone is located below the dissociation limit or not.

4 Conclusions

In this work we have examined the performance of individual (energy-based) configuration selection and energy extrapolation procedures for averaged coupled-pair functional expansions. We have shown that it is possible with the current approach to approximate the complete singles and doubles ACPF energy without significant loss of accuracy and to obtain a better agreement with full CI(FCI) as compared to MRCI without resorting to large amounts of computer time. One

prerequisite for the energy extrapolation to give reliable results is, however, that near-degeneracy effects be treated variationally, i.e., the excitations leading to significant changes in the expansion coefficients are included in the explicitely solved secular equation. Expanding the truncated ACPF in the basis of CASSCF orbitals results in mostly small deviations of the extrapolated energy from the full singles and doubles results. The ACPF energy is found to be slightly more sensitive to the quality of the reference function $|\Psi^0\rangle$ and the size of the selection threshold than the corresponding MRCI results.

The quality of the one-particle density matrix constructed from the truncated ACPF is less satisfactory in the present approach. Computed dipole moments for several electronic states of CuH and PdH show considerable deviations from the values obtained for the densities of non-truncated expansions in some cases. The close resemblance of MRCI and ACPF properties indicates that the effect of unlinked cluster corrections on the dipole moments are lost to a great extent upon configuration selection. It is conceivable, however, that a B_k-type perturbation correction could remedy these shortcomings.

Acknowledgements. C.M.M. wants to thank M.R.A. Blomberg (University of Stockholm) for many valuable discussions on the ACPF approach. Special thanks are due to T. Neuheuser and R. Kluck for their technical assistance in preparing the manuscript. Financial support by the "Deutsche Forschungsgemeinschaft" through SFB 334 is gratefully acknowledged.

References

1. Gdanitz RJ, Ahlrichs R (1988) Chem Phys Lett 143:413
2. Gershgorn Z, Shavitt I (1968) Int J Quant Chem 2:751
3. Buenker RJ, Peyerimhoff SD (1974) Theoret Chim Acta 35:33
4. Buenker RJ, Peyerimhoff SD (1975) Theoret Chim Acta 39:217
5. Bauschlicher CW, Langhoff SR (1987) J Chem Phys 86:5595
6. Marian CM, Blomberg MRA, Siegbahn PEM (1989) J Chem Phys 91:3589
7. Bauschlicher CW, Langhoff SR, Komornicki A (1990) Theoret Chim Acta 77:263
8. Ahlrichs R, Scharf P (1988) Chem Phys Lett 143:501
9. MOLECULE-SWEDEN is an electronic structure program system written by Almlöf J, Bauschlicher CW, Blomberg MA, Chong DP, Heiberg A, Langhoff SR, Malmqvist PA, Rendell AP, Roos BO, Siegbahn PEM, Taylor PR
10. Pople JA, Seeger R, Krishnan R (1977) Int J Quant Chem; Quant Chem Symposia 11:149
11. Epstein DS (1926) Phys Rev 28:695
12. Nesbet RK (1955) Proc Roy Soc (London) 230:312
13. Jenderek J (1990) Diploma thesis, Univ of Bonn
14. The original version of the MRD-CI programs was written by Buenker RJ, Butscher W, Kammer W, Peyerimhoff SD. The currently used system of programs was essentially expanded and modified by Buenker RJ, Chabalowski CF, Chandra P, Engels P, Ernzerhof M, Hirsch G, Heß BA, Jenderek J, Marian CM, Phillips RA
15. The interfaces were written by Ernzerhof M, Marian CM
16. Shepard R, Shavitt I, Pitzer RM, Comeau DC, Pepper M, Lischka H, Szalay PG, Ahlrichs R, Brown FB, Zhao J (1988) Int J Quant Chem; Quant Chem Symp 22:149
17. Werner HJ, Knowles PJ (1991) J Chem Phys 94:1264
18. Roos BO, Taylor PR, Siegbahn PEM (1980) Chem Phys 48:157
19. Cave RJ, Xantheas SS, Feller D (1992) Theoret Chim Acta 83:31
20. Murphy RB, Messmer RP (1992) J Chem Phys 97:4170
21. Marian CM (1991) J Chem Phys 94:5574
22. Marian CM (1990) J Chem Phys 93:1176

23. Lagerqvist A, Neuhaus H, Scullman R (1964) Proc Phys Soc 83
24. Balasubramanian K, Feng PY, Liao MZ (1987) J Chem Phys 87:3981
25. Rohlfing C, Hay PJ, Martin RL (1986) J Chem Phys 85:1447
26. Langhoff SR, Petterson LGM, Bauschlicher CW (1987) J Chem Phys 86:268
27. Heß BA (1992) Phys Rev A33:3742
28. Bauschlicher CW (1982) Chem Phys Lett 91:4
29. Engels B (1991) Chem Phys Lett 174:398
30. Banichevich A, Peyerimhoff SD, Chem Phys (in press)
31. Karlström G, Engström S, Jönson B (1978) Chem Phys Lett 57:390
32. Lee TJ (1990) Chem Phys Lett 169:529
33. Tanaka T, Morino Y (1969) J Mol Spectrosc 32:538
34. Almlöf J, Taylor PR (1987) J Chem Phys 86:4070
35. Shih SK, Buenker RJ, Peyerimhoff SD (1974) Chem Phys Lett 28:463
36. Burton PG (1979) J Chem Phys 71:961
37. Hay PJ, Dunning TH (1977) J Chem Phys 67:2290
38. Wilson CW Jr, Hopper DG (1981) J Chem Phys 74:595
39. Wright JS, Shih SK, Buenker RJ (1980) Chem Phys Lett 75:513
40. Jones RO (1985) J Chem Phys 82:325
41. Moscardó F, Andrias R, San-Fabián E (1988) Int J Quant Chem 34:375
42. JANAF Thermochemical Tables (1971) 2nd edn, Washington
43. Borowski P, Andersson K, Roos BO (1992) J Chem Phys 97:5568
44. Werner HJ, Knowles PJ (1988) J Chem Phys 89:5803
45. Siegbahn PEM. An internally contracted ACPF program
46. Werner HJ, Knowles PJ (1990) Theoret Chim Acta 78:175
47. Jackels CF, Shavitt I (1981) Theoret Chim Acta 58:81